

# Towards predictive engineering-type simulations of upward flame spread in SBI scenarios

**Georgios Maragos, Alexander Snegirev, Jeri At Thabari, Youk Moorthamers, Bart Merci**

Department of Structural Engineering and Building Materials, Ghent University, Belgium.

E-mail: Georgios.Maragos@UGent.be

**Abstract.** Focusing on advancing predictive modelling of upward flame spread using CFD, large eddy simulations using FireFOAM are presented. A fully dynamic approach with respect to turbulence, combustion and radiation, as well as modelling convective heat transfer based on Newton's law with simplified correlations for natural convection, is considered. The thermal decomposition of the solid material is modelled using a 1D pyrolysis model combined with optimised model-effective material properties. For validation purposes, a series of medium-scale Single Burning Item (SBI) experiments using both inert (calcium silicate) and flammable walls (plywood) is considered. Separate validation of the gas (pool fires) and solid (anaerobic pyrolysis) phases is also reported. A comprehensive comparison between the CFD model predictions and available experimental data is performed. The modelling approach performs very satisfactorily with the predictions being rather grid-insensitive and resulting in maximum deviations in the predicted HRR, between the coarsest and finest grid size, on the order of 15%.

## 1. Introduction

In order to assess fire safety, all building components have to be assessed according to certain standards. Fire testing is used for determining whether a product meets the minimum requirements as set out in national building codes and standards. Upon successful completion of a fire test by nationally accredited laboratories, materials get certified based on their reaction-to-fire behavior. Reaction-to-fire testing is a mandatory requirement of building codes and regulations in all European countries, one of these tests being the intermediate-scale EN 13823 [1] test for building products which is also the focus of the current paper.

Nowadays, the fire behaviour of building materials can also be tested through the use of Computational Fluid Dynamics (CFD) which is used as supplementary to experimental tests in order to gain further insights and to potentially reduce the number of actual tests and the high costs associated with experimental campaigns. A methodology for model validation (see Figure 1(a)) is needed in order to develop a reliable and accurate CFD framework for modelling flame spread scenarios. A fundamental understanding of the different physical phenomena involved in flame spread scenarios is crucial and many challenges need to be addressed before developing accurate models that could be used in predictive fire modelling. More specifically, there is an intricate coupling of the different physics involved in the gas phase, which cannot be easily decoupled, and provide the necessary heat feedback to the fuel surface which determines the rate of solid pyrolysis and the subsequent flame spread (see Figure 1(b)).

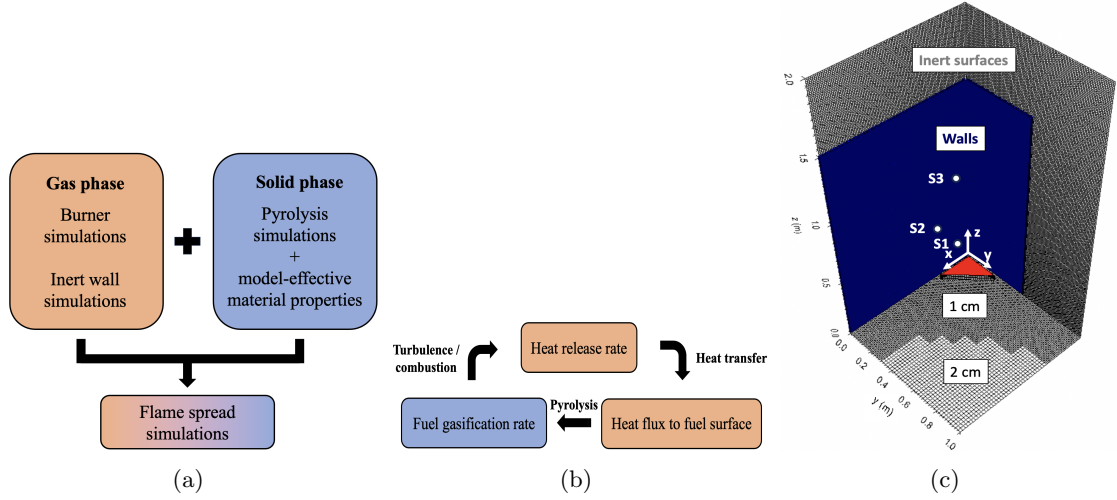


**Figure 1.** Illustration of the (a) methodology used for model validation, (b) gas-solid phase coupling in flame spread scenarios and the (c) domain used in the simulations. Blue color: plywood walls, red color: burner. The location of the gauge heat flux sensors S1 ( $x = 0.08$  m,  $z = 0.21$  m), S2 ( $x = 0.2$  m,  $z = 0.35$  m) and S3 ( $x = 0.08$  m,  $z = 0.8$  m) is also depicted.

The present work reports on LES simulations of fire growth in Single Burning Item (SBI) scenarios and aims to enhance (predictive) fire modelling when it comes to simulating upward flame spread. A stair-step validation approach is employed by considering pool fire experiments (only gas phase), anaerobic pyrolysis experiments (only solid phase) as well as SBI experiments (coupling between the gas and solid phase) involving both inert (calcium silicate) and flammable (plywood) walls. The focus of the study is explicitly on grid sizes that are sufficiently small for resolving reasonably well the fire plume dynamics but that are not fine enough to accurately resolve the boundary layer (i.e., grid sizes often used for engineering-type of simulations).

## 2. Experimental test cases

A brief overview of the various experiments used for validation of the simulations is presented here. The medium-scale  $C_3H_8$  pool fire experiments (i.e., 20.7, 34.4 and 50.1 kW), involving a 37 cm in diameter circular burner, by Falkenstein-Smith et al. [4], are considered for validation purposes in the gas phase. A series of anaerobic pyrolysis experiments of plywood samples (i.e., 0.0953 m in diameter and 0.0169 m in thickness), performed in the Fire Propagation Apparatus (FPA) [5], are used for validation purposes in the solid phase. A series of SBI experiments [6], involving a 30 kW triangular  $C_3H_8$  burner and 1 m x 1.5 m calcium silicate / plywood walls, are used for validation purposes of the gas - solid phase coupling modelling approach.

## 3. Modelling

The CFD code FireFOAM, developed by FM Global, is used here. A fully dynamic approach is used for modelling, turbulence (dynamic Smagorinsky), combustion (EDM) and radiation (gray version of WSGG with a dynamically-calculated path length) [2], convective heat transfer is modelled based on Newton's law using simplified correlations for natural convection [3], while a single-step Arrhenius type of pyrolysis model, combined with optimised model-effective material properties [5], is used for solid decomposition. To avoid added complexity, modelling of char oxidation is not considered in the present study, however, its influence will be explored in the future. The experimental measurements in [4], served as a reference for estimating the radiative

emission (0.33) of the gaseous burner in the SBI scenarios. The radiative emission (0.3) for plywood was assumed the same as pine wood and was taken from the literature.

A computational domain of  $1\text{ m} \times 2\text{ m} \times 1\text{ m}$  ( $L \times H \times W$ ) is used to model all SBI scenarios (see Figure 1(c)). Two different wall materials are considered including both inert (calcium silicate) and flammable (plywood) surfaces. The considered grid sizes include 4 cm, 2 cm and 1 cm with the gas phase cells mapped onto the solid walls. Through the thickness of the walls, 30 and 45 cells are considered for the inert and flammable walls, respectively. A 30 kW propane triangular burner with a prescribed time ramp to reach the maximum HRR after 30 s, according to the experiments [6], is the initial fire source.

## 4. Results

### 4.1. Pool fire simulations

The predicted centerline temperatures, with  $z$  the axial distance and  $D^*$  the characteristic fire diameter, are presented in Figure 2. The error bars represent a 10% uncertainty in the experimental measurements. Overall, the model predictions are rather grid-insensitive and in very good agreement (i.e., lie within the experimental uncertainty) with the experimental data for the range of heat release rates considered. This is a consequence of the dynamic modelling approach considered in the gas phase. The very steep temperature gradients observed in the experimental measurements, just above the fire source, are captured reasonably well by the simulations regardless of the grid size. Depending on the grid size, the predicted radiative fractions were reasonably well-predicted and within 0.5 - 4% of the desired experimental values.

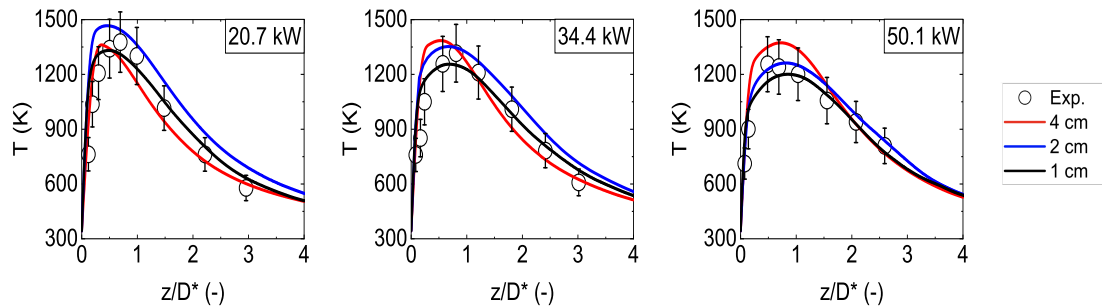


**Figure 2.** Predicted centerline temperature for  $C_3H_8$  pool fires with various heat release rates.

### 4.2. Pyrolysis simulations

Figure 3 presents results from pyrolysis simulations of plywood samples under different heat fluxes. Overall, the agreement between the experimental data and the simulation results is reasonable. The simulations are able to capture fairly well the main experimental trends (i.e., double peak in the mass loss rate as well as the sharp increase of the surface temperature). However, some discrepancies do exist in both cases (i.e., lower mass loss rate in the second peak and lower final backside temperatures), which are more pronounced in the lower heat flux cases considered. In general, the first peak observed in the mass loss rate results depends on the boundary conditions and the applied heat flux on the sample surface. In most cases, these are correctly captured by the simulations. The second peak, however, occurs after heat has penetrated from the char layer formed at the top surface during the initial stages of the pyrolysis and can be affected by the backside boundary conditions. In general, discrepancies are observed in the predicted backside temperatures towards the end of the tests for both materials. As reported in [5], exposure of the thermocouples and the back-boundary to heater radiation

through cracks in the samples could partially contribute to these discrepancies. Other possible reasons include the consideration of temperature-independent material properties, the pyrolysis model not accounting for water evaporation or moisture mitigation to the backside of the sample as well as no modelling of cracking or delamination of the samples.

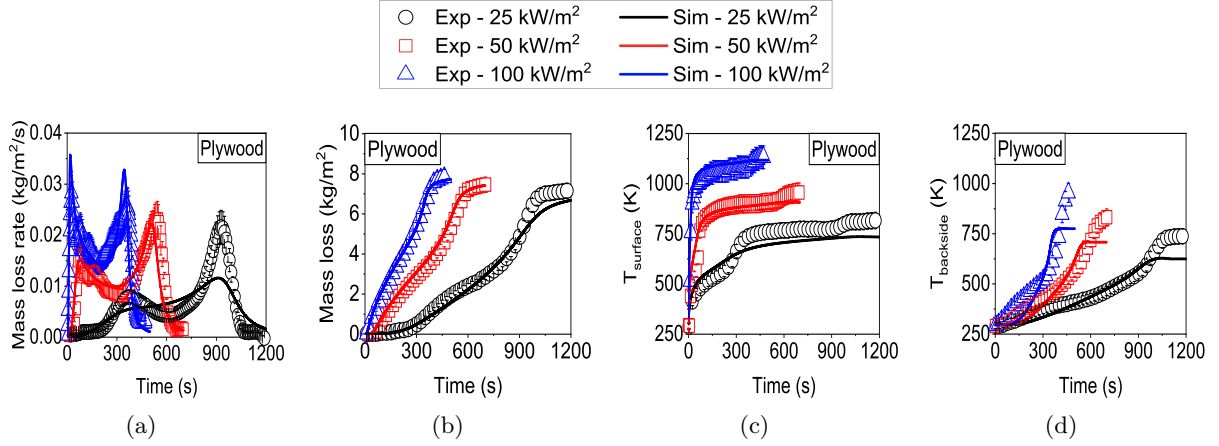


**Figure 3.** Predicted (a) mass loss rate, (b) mass loss, (c) surface temperature and (d) backside temperature in pyrolysis simulations of plywood samples.

#### 4.3. Inert wall simulations

A comparison between the predicted total heat fluxes in inert wall scenarios is presented in Figure 4. The predicted radiative fractions from the simulations are approximately 33.2%, 32.9% and 33.7% for the 4 cm, 2 cm and 1 cm grid size cases, respectively, all very close to the desired value of 33% for the burner [4]. The employed modelling approach can, therefore, guarantee that the correct amount of radiation is released, regardless of the grid size used, which is a prerequisite for accurately predicting the heat feedback on the wall surface. The flame heights from the simulations are estimated based on the criterion of the integrated heat release rate per unit volume (taken here as 97%) with the predicted values being approximately 0.74 m, 0.87 m and 0.89 m for the 4 cm, 2 cm and 1 cm grid size cases, respectively. Hence, the 2 cm and 1 cm grid size simulations are able to approximately replicate the experimentally reported flame height of 0.87 m [6], while the 4 cm grid size scenario still remains fairly close.

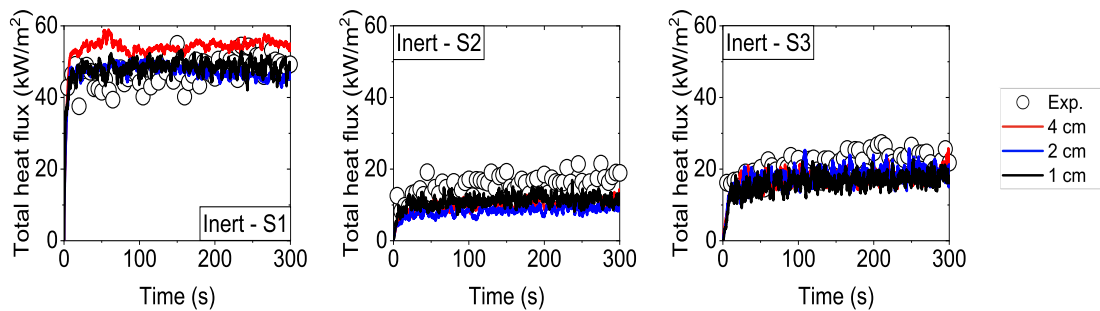


**Figure 4.** Total heat fluxes at sensors S1 - S3 in the inert wall simulations.

The observed differences in the predicted flame heights lead, however, to some differences in the flame structure as a function of grid size (i.e., flames having bigger volume and being

more concentrated near the corner with the 4 cm grid size) and influence locally the spatial distribution of the heat feedback to the fuel surface. More specifically, higher incident heat fluxes, up to 10 - 15 kW/m<sup>2</sup>, are obtained for the coarsest grid size (4 cm) case compared to the finer grid cases (2 cm and 1 cm) at sensor S1. The 4 cm grid size case, even though being fairly coarse, predicts a initially convective heat fluxes on the order of 10 kW/m<sup>2</sup>, decreasing to approximately 5 kW/m<sup>2</sup> towards the end of the simulation since the walls are heating up and  $\Delta T$  decreases. The finer grid size cases (2 cm and 1 cm) on the other hand, resolving better the boundary layer near the wall surface, predict higher convective heat fluxes (i.e., initially on the order of 15 kW/m<sup>2</sup>, decreasing to approximately 5 kW/m<sup>2</sup> towards the end of the simulation for the same reason explained previously). This also results in a slight decrease of the total heat fluxes observed at this location, as a function of time. On the other hand, minor differences are observed at sensors 2 and 3 with the total heat fluxes being fairly close to the experimental measurements in most cases. Overall, and for the reasons discussed above, fairly grid insensitive predictions for the total heat fluxes are obtained for the simulations with the finer grid sizes (2 cm and 1 cm), but not with the coarsest one (4 cm). It is worth noting that the total heat fluxes often tend to be under-predicted on coarse grid simulations because either the radiative fractions, hence, the radiative heat fluxes are under-predicted and / or the convective heat fluxes are not well-resolved. However, this is not the case in the present simulations with any of the grid sizes considered since both the correct amount of heat due to radiation is released (at least globally) and the convective fluxes do not exhibit strong grid-dependency.

#### 4.4. Flammable wall simulations

The predicted total heat release rates (i.e., added contributions from both the burner and the flammable walls) from the simulations with the flammable plywood walls is presented in Figure 5. Given the range of grid sizes used in the simulations (i.e., 1 - 4 cm), the heat release rate predictions are surprisingly grid insensitive and are able to follow the experimental trends in most cases. As expected, higher heat release rates are obtained with decreasing grid cell size due to better resolution of the flame structure and temperature which increases the, overall, heat feedback to the wall surface. The gradual increase in the HRR until it reaches a plateau at approximately 30 kW is due to the C<sub>3</sub>H<sub>8</sub> burner alone. During this period there is pre-heating (due to convection and radiation) of the flammable walls which eventually leads to pyrolysis gases being released, the walls to be ignited and the flames to eventually spread both axially and laterally at different rates.

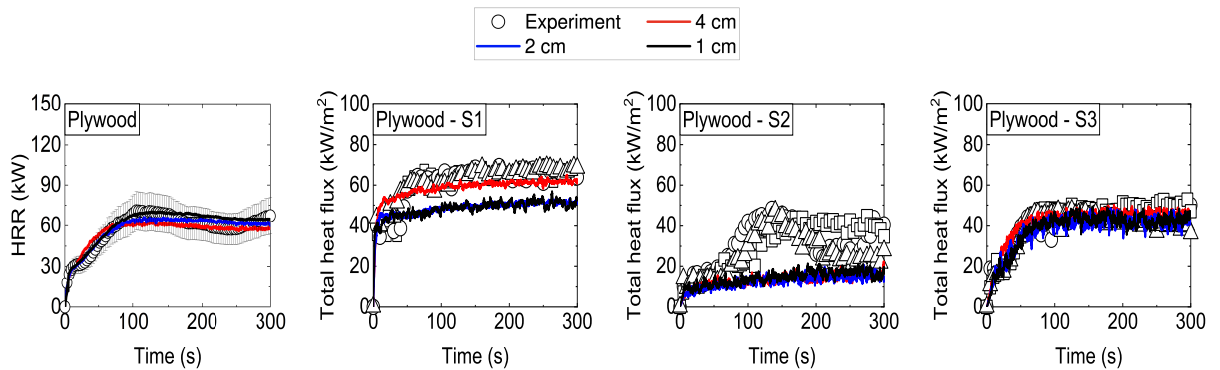


**Figure 5.** Total heat release rate (burner and walls) and total heat fluxes at sensors S1 - S3 in the flammable wall simulations.

To aid the analysis of the results, the total heat fluxes at sensors S1 - S3 are also presented. The simulation results follow the major trends observed in the experimental measurements.

More specifically, a very fast increase in the total heat fluxes is observed at sensor S1 since flames are consistently present in this location from the start of the simulations. The maximum predicted heat fluxes are on the order of  $60 \text{ kW/m}^2$  for the coarsest grid size (4 cm) while approximately  $50 \text{ kW/m}^2$  for the finer grid sizes (2 cm and 1 cm). This decrease in the total heat fluxes is due to differences in the flame structure which affect the incident heat fluxes at this location (as previously also explained in the inert wall simulations). The experimental measurements in this case lie between  $60 - 70 \text{ kW/m}^2$ , values which are actually higher than measurements taken with MDF walls that burned more intensively than plywood (i.e., with the total heat flux predictions on the order of  $60 \text{ kW/m}^2$  [6]). Given these aspects, it should not be excluded that there might be some discrepancies in the experimental measurements in this case. A gradual increase in the total fluxes is predicted at sensor S3 which is initially mainly to convection (pre-heating the wall) until the flames grow in size, spread upwards and radiation becomes dominant. The maximum obtained values from the simulations are on the order of  $40 - 45 \text{ kW/m}^2$  and remain close to the experimental measurements. A steady and gradual increase in the total heat fluxes is also predicted at sensor 2. However, the distinct peak observed in the experiments due to lateral flame spread and the flame front passing from this location is not observed in the simulations. This aspect could potentially be partially attributed to the 1D heat transfer model not accounting for conductive heat transfer in the lateral directions.

## 5. Conclusions

Large eddy simulations of upward flame spread in Single Burning Item (SBI) scenarios with FireFOAM were presented. The model was extensively validated by simulating the gas (i.e., gaseous pool fires) and solid (i.e., anaerobic pyrolysis) phases separately, as well as coupled simulations of medium-scale SBI scenarios considering inert (calcium silicate) and flammable (plywood) walls. The study explicitly focused on flame spread simulations involving grids that are sufficiently small to capture the fire plume dynamics but not to accurately resolve the boundary layer near the walls. Given the complexity of the problem, the employed modelling approach led to reasonable and rather grid-independent predictions, when compared to available experimental data, as a function of grid size (i.e., in the range of 1 - 4 cm) for a range of scenarios considered. Overall, the performance of the approach was very satisfactory (i.e., maximum deviations in the predicted HRR, between the coarsest and finest grid size, on the order of 15%) and illustrated the potential of CFD to accurately model upward flame spread scenarios even if the boundary layer is not (fully) resolved in the simulations.

## Acknowledgments

This research is funded by The Research Foundation – Flanders (FWO – Vlaanderen) through project G023221N.

## References

- [1] EN 13823, Reaction to fire tests for building products - Building products excluding floorings exposed to the thermal attack by a single burning item, European Standard, 2014.
- [2] G. Maragkos, B. Merci, On the use of dynamic turbulence modelling in fire applications, *Combust. Flame* 216 (2020) 9-23.
- [3] F.P. Incropera, D.P. DeWitt, T.L. Bergman, A.S. Lavine, *Fundamentals of Heat and Mass Transfer* (6th edition), John Wiley & Sons, USA, 2006.
- [4] R.L. Falkenstein-Smith, K. Sung, A. Hamins, Characterization of Medium-Scale Propane Pool Fires, *Fire Technol.* 59 (2023) 1865-1882.
- [5] G. Agarwal, M. Chaos, Y. Wang, Validation of pyrolysis model in transient heating scenarios and diverse spectral boundary conditions, *Fire Saf. J.* 120 (2021) 103064.
- [6] D. Zeinali, Flame spread and fire behavior in a corner configuration, PhD thesis, Ghent University, 2019.